Open Access

SCHOLARENA

Journal of Innovations in Energy science

RESEARCH ARTICLE

IOT Remote Monitoring of a Wind Turbine Backed Up by Electrical Grid

Djohra Saheb[1*], Abdessalem Bouferrouk[2] and Mustapha Koussa[1]

[1]Division Energie Solaire Photovoltaique, CDER, Algiers, Algeria

[2]School of Engineering, University of the West of England, Bristol, BS16 1QY, UK

[*]**Corresponding author:** Djohra Saheb, Division Energie Solaire Photovoltaique, CDER, Algiers, Algeria, Tel: +213559884865, E-mail: dkoussa@cder.dz; d.saheb@cder.dz

Citation: Djohra Saheb, Abdessalem Bouferrouk, Mustapha Koussa (2022) IOT Remote Monitoring of a Wind Turbine Backed Up by Electrical Grid. J Innovations Energy Sci 2: 105

Abstract

This paper presents the design, practical implementation and remote monitoring of a small wind turbine backed up by electrical grid. The wind turbine, installed on the Bouzaréah site in Algiers, is remotely monitored via Internet of Things (IoT) in order to perform supervisory tasks, control energy demand, and acquire environmental and performance data. The IoT system allows users to gather weather data, acquire operating parameters, access energy performance details, and perform energy manager duties. The most important advantage of the developed software tool is its fluidity in remote control without slowing. The produced electricity is sufficient for lighting ten lamps of 60W each, consuming a total current of 2.8A. The obtained results demonstrate the successful working of the remotely controlled wind turbine, and show the potential for onsite supervision and acquisition of meteorological and electrical data by the developed IoT-based setup. The IoT-based setup will be used to observe the long-term behavior of the wind turbine, to validate the power curves, to optimize performance, and to create a database for further research on larger-scale wind turbines and other renewable energy systems. Developments like these fit within Algeria's ambition to generate 25 GW of electricity from renewable sources by 2030.

Keywords: Remote Monitoring; Micro Wind Turbine; Electrical Grid; Data Acquisition; Monitoring; Supervision; Internet of Things (IOT)

Introduction

According to IEA [1] and in relation to the Covid-19 pandemic, there were lower demand forecasts for oil, coal and gas consumption by 9%, 8% and 5%, respectively. As a consequence, there was a net reduction in emissions of harmful gases, including CO2, which decreased by 8% in 2020 alone. It is anticipated that the harmful emissions will decrease by at least 55% by 2030 [1]. Furthermore, and according to the same publication, use of renewable energies grew by 1.5% during the first quarter of 2020. The most relevant reason for this growth is that, on the one hand, the production of electricity from renewable sources is much cheaper in the long term than that produced by conventional power plants. On the other hand, in order to encourage the energy transition to zero-emission systems many regulators make renewable energy production for the grid injection a key priority [1].

In Algeria, the use of renewable energy has not previously been an essential part of the country's national energy program, while today there is an undisputed awareness by all policy-makers and individuals of the serious prospects of this resource. This is linked on the one hand to the fossil-fuel energy resources depletion, and on the other hand to the concerns brought about by climate change.

The target for Algeria's renewable energy program is to generate 25 GW of electrical power from renewable sources by 2030, of which 5010 MW will come from wind energy alone [2]. In support of the Algerian energy program, several studies are found in the literature that inform and develop knowledge around renewable energies, from a technical and economic viewpoint [3-16]. However, one of the key technology drivers, often not sufficiently considered in these studies, is the real-time remote monitoring and supervision of renewable energy systems to improve performance. In [17], the authors adopted an OPC Unified Architecture as a protocol of communication, which was implemented in the gateway, in order to facilitate the link between OPC UA client and IBM cloud. In another paper [18], an FPGA-CPU based holistic monitoring system was proposed which not only provided both condition and SSCI monitoring functions simultaneously in real-time but also recorded necessary data for post-event analysis. Chandra et al. [19] proposed Cloud based real-time monitoring and control of a diesel generator using the Internet of Things (IoT) technology and in [20] wind characterization for a three blade Savonius wind turbine (WT) using IoT was studied. Various challenges, including materials for the wind turbine and methods of condition monitoring were discussed and the results were analyzed with statistical measures and compared with standard values. In a further study [21], the authors explored various areas of IoT application with respect to WT system such as IoT integration with energy generation system, IoT in wind turbine monitoring and control, maintenance, and prediction systems. An Intelligent Smart Energy Management Systems (ISEMS) was proposed in [22] to handle energy demand in a smart grid environment with integration of renewables energies. One of the long-standing limitations of clean energy tech**nology** has been the inherent vulnerability of the physical infrastructure, which is often located in harsh outdoor environments. Before wind energy can replace fossil fuels as the world's primary sources of power, these systems must be able to offer the stability needed to provide power to both residential and commercial buildings. This is where IoT can make real difference [23], particularly in terms of **asset monitoring, automated controls and data analysis.** The demand for renewable energy systems that can be smartly managed using IoT is growing.

Within this context, the main objective of the present paper is the development and onsite implementation of a real-time remote supervision and data acquisition system for a small-power wind turbine, backed up by the electrical grid. A grid-connected wind power system is more preferred over standalone machines in order to guarantee an uninterrupted supply of electric power. The developed software tools for the system allows weather data logging and acquisition of operating parameters as well as performing the duties of an energy manager. The most important advantage of the developed software is its fluidity in remote control without slowing. Achieving this objective requires the development of hardware and software, and knowledge of wind energy, electricity, electronics and IoT. The different equipment and tools that need to be integrated for the developed system are: (1) measuring instruments to measure meteorological data and the different electrical operating parameters, (2) the circuits for conditioning the analog signals as received by the measuring instruments (thus helping to provide precise measurements), (3) an analog to digital converter, which converts the analog signal into a digital form, before the data is transferred to the microcomputer where it is stored and finally transmitted to a web server, and (4) the data provided requires use of graphic pages and Excel files as data formats.

System configuration and components

The wind power system, which is usually backed up by the national electrical grid (or a diesel generator when the grid is down), is implemented at the Centre de Développement des Energies Renouvelables (CDER)- Centre for Development of Renewable Energies- located in the celeste village of Bouzaréah in the western suburbs of Algiers, Algeria. The wind power system that is currently installed at CDER and electrifies part of its energy network is a micro-grid type, model Whisper 200, and is shown in Figure 1.

Figure 1: The Whisper 200 wind generator, backed up by electrical grid as installed at CDER.

The whole system considered in this paper consists of the following components.

Whisper 200 micro wind generator

The whole system, which consists of a wind generator and a charge regulator (Figure 2 a & b), converts wind energy into direct current through the charge regulator. It is designed to operate on sites with low to medium average wind speeds (3.6 m/s and more). Its peak electrical power is 1 kW, achieved at the rated wind speed range of 11.6 m/s to 13 m/s.

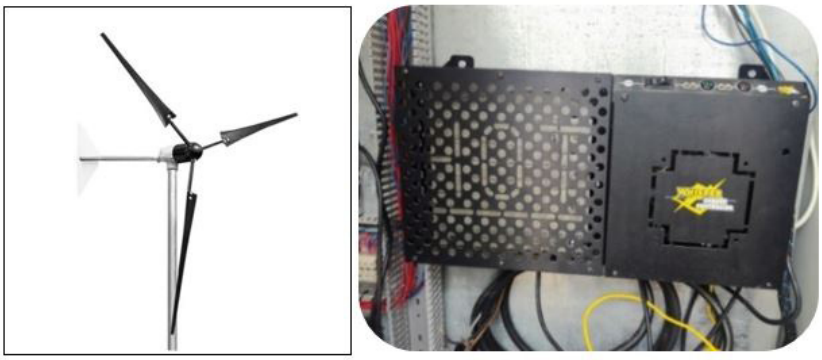

Figure 2: The Whisper 200 parts: (a) wind generator, and (b) charge regulator

Storage system

For the storage system, shown in Figure 3, the 2V Hoppecke stationary solar batteries 10 OPzS 1000 are used. These batteries are connected in series of 12 because the installation is 24 V, and the batteries are connected between the load controller and the inverter.

Figure 3: Storage system in the form of 12 Hoppecke stationary solar batteries

The AJ sine wave inverter co

Inverter

Inverts the DC voltage of batteries into a pure *sine wave AC voltage* output with a power of 1.3 kVA for 24 V. The inverter is shown in Figure 4 (a).

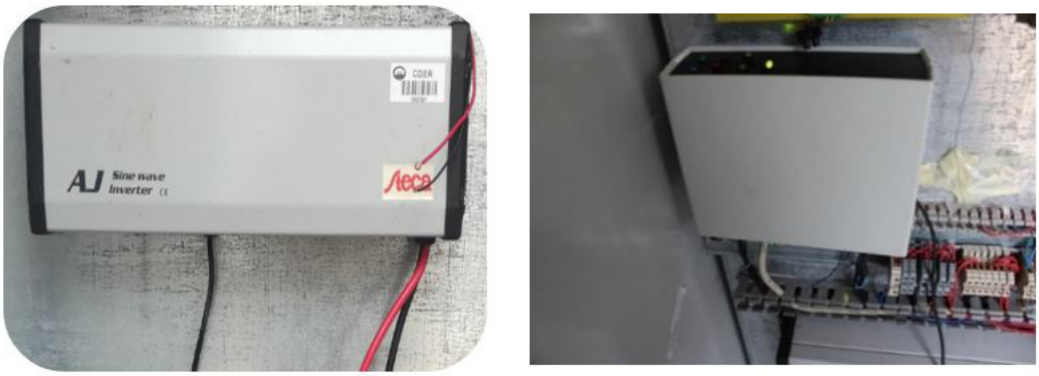

Figure 4: Electrical subsystems: (a) the AJ sine wave inverter, (b) the energy manager

Energy management system (energy manager) [24]

The energy manager (pictured in Figure 4 (b)) allows intelligent energy management coming from the wind generator and the grid, or diesel generator, promoting the use of free and clean renewable energy resource. It works with the system structure to allow smooth electric power supply distribution without interruption. The three main operating modes are:

• Favorable: where the wind energy production stored in the batteries is greater than consumption and therefore the manager directs the surplus energy to the grid;

• Neutral: where the wind energy production is just sufficient for the load consumption;

• Unfavorable: where the wind energy production is less than the load consumption. In this case, the energy manager directs the power from the grid (or the diesel generator) such that it behaves as an additional source of power.

The energy management system functions in three steps as follows:

First step: Using sensors the management system measures three voltages: that of the batteries (V_{batt}), and that of the electrical grid (V_{grid}) .). This information is processed according to a management flowchart shown in Figure 5. At the end of the processing of this information, decisions are taken in the direction of an effective management of the produced energy (Figure 5).

Figure 5: First step of management system working

Second step: Knowing the value of the state of charge (SOC) of the batteries, the energy management of the system works as follows (see Figure 5). If the state of charge of the batteries is between the SOC min and the SOC max this means that the batteries are charging the controller commands by closing of the relay placed between the load and the batteries, which allows the load to be powered by the batteries through the inverter and also allows the batteries to be charged by the wind system. If, however, the SOC is greater than the SOC max, the load is still powered and the excess energy will be dissipated as heat either through an electrical resistance, or as energy injected to the grid. This operation is controlled by the charge regulator (Figure 6).

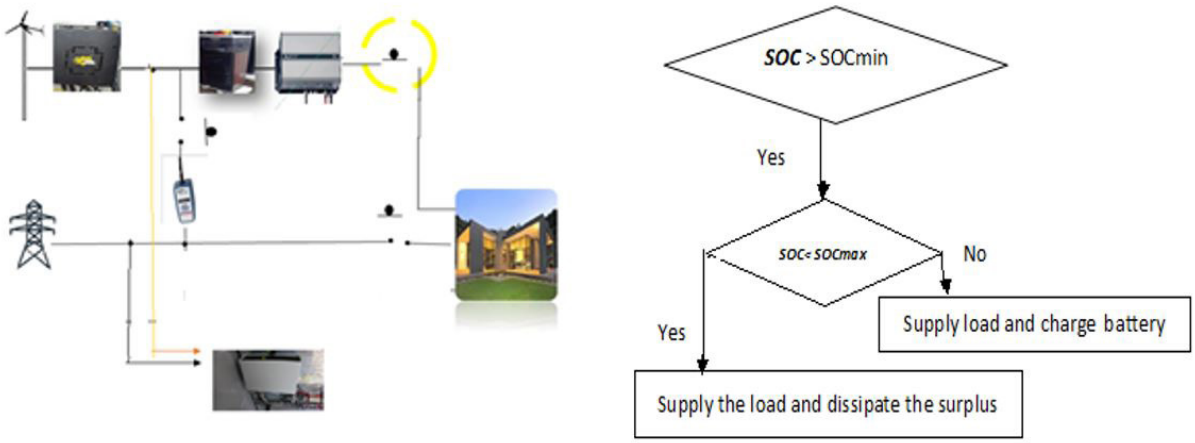

Figure 6: Second step of management system working

Third step: If the batteries state of charge is lower than the value of the SOC min a test on the availability of network must be carried out. If the network is available then the relay located between the load and the network will be closed to supply the load while at the same time, a second relay is closed on to also charge the batteries (Figure 7).

If the electrical grid does not exist then an audible alert is triggered to indicate the absence of energy source, as indicated in the Flowchart of Figure 7.

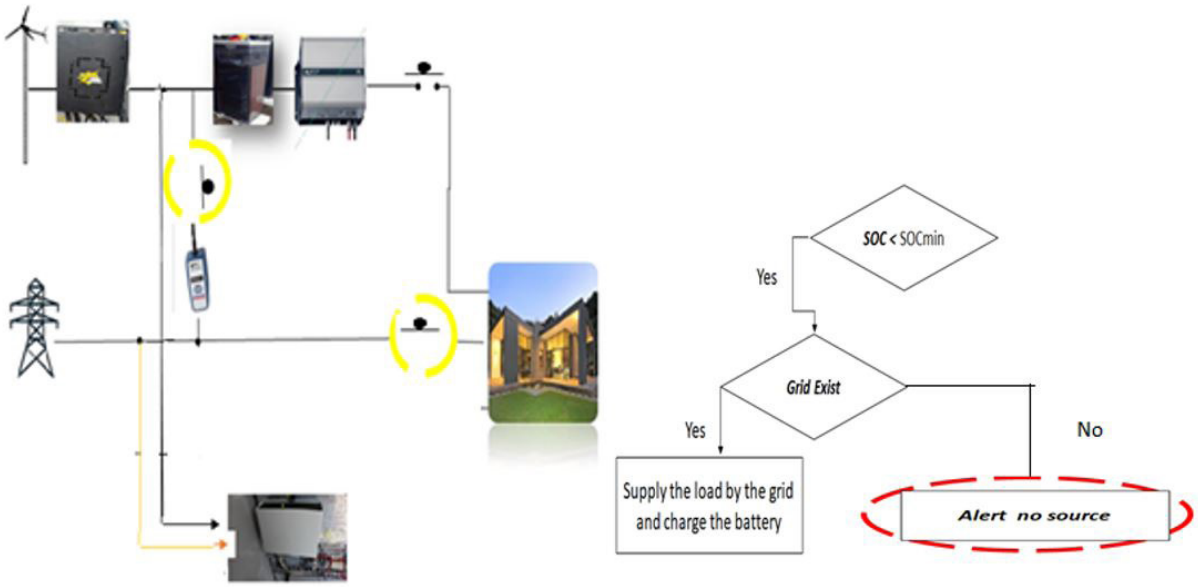

Figure 7: Third step of management system working

Protection system

It allows isolating and protecting the energy manager, ensuring a separation between the "command" and the "power".

Inverter / charger

The power of this device is 3 kVA / 24V with a digital display communication card that combines a pure sine wave converter, an MPPT solar regulator and a battery charger. In the present case, this unit is exploited as a battery charger where the order to charge comes from the energy manager system cited above. The characteristics of the inverter/charger are illustrated in Table 1. The functions performed by the inverter/charger include:

- Charging current is controlled and shuts off when the batteries are fully charged;
- Setting the battery charging algorithm;
- Battery discharge limitation in stages

Date	Value
Input AC	90-280 V
Float charge voltage (Vcc)	27 V
Max. Cut-off voltage	30 V
Max charging current	30 A

Table 1: The Inverter / charger characteristics

Data acquisition of operating parameters

The AGILENT 34970 (Figure 8) is the data acquisition device used to acquire operating parameters related to system performance such as voltages, currents and temperatures. These data are recorded and stored in Excel files for easy use and handling.

Weather data logger

The design and implementation of the meteorological parameters acquisition card were developed at CDER [25]. This card is used to measure and display wind speeds and direction, relative humidity, temperature and pressure. All these parameters are

transferred to a memory card. The main characteristics are a measurement interval of 5 minutes and data recording in ".dat" files format. The goal of the weather data logger is to show the influence of meteorological parameters (e.g. wind, temperature, pressure and humidity) on the power production from the Whisper 200 wind generator. This will allow users to perform modeling and numerical simulation of power production, taking into account the effects of meteorological parameters.

Figure 8: Data acquisition system for the meteorological data

Graphical interface

The development of a graphical interface (Figure 9) using GUI / MATLAB software allows local supervision and control of the devices used for the production and storage units of the wind generator / grid / battery experimental platform installed onsite. It also supervises the actual management of all these means of energy production and storage in order to optimize the services provided to the end user.

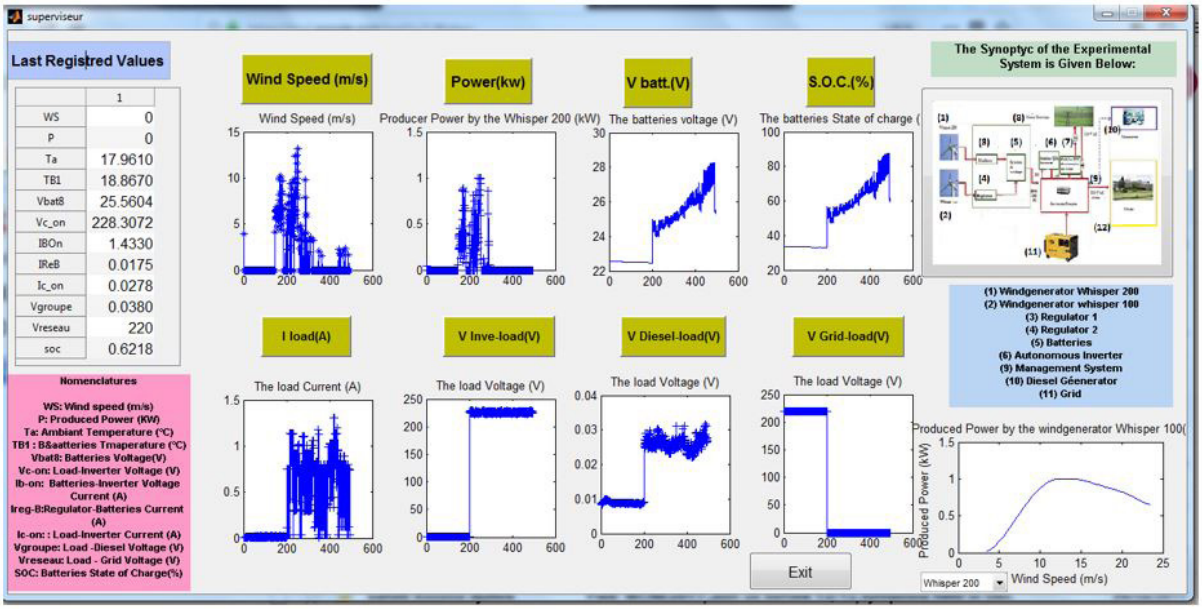

Figure 9: Graphical interface system (GUI/MATLAB) for diagnostics and supervision

Graphical monitoring software

To remotely access the graphical monitoring software (Figure 10) installed on the PC's desktop at the experimental platform, AnyDesk software was exploited. Once activated and configured, it allows access to files and applications on the remote computer from any web browser. The most important advantage of the AnyDesk software is its fluidity for remote control without slowing down data transfer.

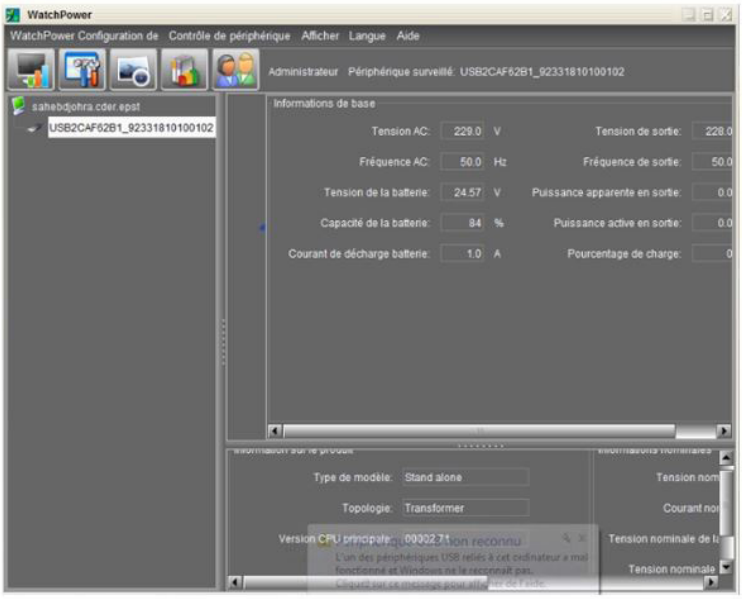

Figure 10: The graphical monitoring software for remote access

Functional description of the system and meteorological parameters

The system has been sized to allow the study of a real case electricity production from wind energy. It operates in one of the following two modes:

- Exploitation of the produced electricity for lighting use onsite;
- Possibility of connection to the grid with injection of the surplus power production;

Site meteorological parameters

The mechanical power produced by the wind generator is given by equation (1):

$$P_w = \frac{1}{2}\,\rho\, S\; V^3\, C_p(\lambda,\beta) \tag{1}$$

where ρ is the air density (kg/m^3), S is the surface area swept by the blades (m^2), V is the average wind speed (m/s) at the site, C_p is the power coefficient of the wind generator as a function of the tip speed ratio (λ) and the blade setting angle (β). Air density ρ is taken to be 1.225 kg/m^3 at 15 °C at sea level. More generally, the density of dry air and at height h is given as 626[26]:

$$\rho(h) = \frac{P(h)}{R\; T(h)} \tag{2}$$

where $P(h)$ is the atmospheric pressure at altitude h (in Pa), R is the ideal gas constant for air (R = 287 Jkg^{-1}K^{-1}), and $T(h)$ is the temperature at altitude h (in K). Hence, the formula for dry air density becomes:

$$\rho = \frac{P}{287.06 \times (\,273.15 + T)} \tag{3}$$

Thus, the power of the turbine in conditions of dry air becomes:

$$P_w = \frac{1}{2}\,\frac{P}{287.06 \times (273.15+T)} \times S \times V^3 \times C_p(\lambda,\beta) \tag{4}$$

To give a more precise value of the air density, the humidity should be considered because it influences the specific constant of the

humid air R_h. The humid air density is expressed as:

$$\rho = \frac{P}{R_h \times (273.15+T_a)} \quad (5)$$

where the specific constant of the humid air R_h is expressed as:

$$R_h = \frac{R_s}{1-\left(H_r \times \frac{P_{sat}}{P}\right)\times\left(1-\frac{R_s}{R_v}\right)} \quad (6)$$

where R_s is the specific constant of dry air equal to 287.06 J kg^{-1} K^{-1}; R_v is the specific constant of water vapor equal to 461 J kg^{-1} K^{-1}; H_r is the relative humidity as a %; P is the air pressure in Pa, and P_{sat} is the saturated vapor pressure of water in the air, determined by Magnus' formula [26] as in equation 7:

$$P_{sat} = 611.213 \times e^{\left(\frac{17.5043 \times T_a}{241.2+T_a}\right)} \quad (7)$$

where T_a is the ambient temperature in °C. This formula is valid for -30°C < T < 70 °C and gives the pressure in Pascal. Hence, finally, the air density model is given by equation 8 and the wind generator power produced is given by equation 9.

$$\rho(H_r, T_a, p) = \frac{1}{287.06 \times (273.15 + T_a)}\left(p - 230,616\ H_r\ e^{\left(\frac{17.5043 \times T_a}{241.2+T_a}\right)}\right) \quad (8)$$

$$P_p(H_r, T_a, p) = \frac{1}{2}\frac{1}{287.06 \times (273.15 + T_a)}\left(p - 230,616\ H_r\, e^{\left(\frac{17.5043 \times T_a}{241.2+T_a}\right)}\right) SV^3 C_p(\lambda, \beta) \quad (9)$$

Results and discussion

Impact of the site meteorological parameters on productivity

The data in Figure 11 show the variations of absolute humidity, pressure, density and temperature during a typical 24 hours period (00:00 to 24:00) in February 2021, as recorded by the data acquisition system. The data reveal that:

• The air density and the pressure vary in the same direction such that the minimum values are reached at 9 p.m. and the maximum values are reached at 6 a.m. and 7 p.m. This is explained by the fact that, if the air pressure or absolute humidity increases or decreases then this affects directly the air specific volume, which consequently decreases, or increases according to the pressure or absolute humidity evolution; hence, the air density increases also;

• According to the thermodynamic law, from results presented in Figure 11, it is observed that the temperature and absolute humidity vary in the opposite direction. So, the opposite is observed between 9 p.m. and 12 p.m. This is linked to the pressure decreasing during this period, which is linked also to the wind speed evolution.

In Figure 12 are presented the hourly variations of the wind speed, power produced by the wind generator, and the air density. These curves reveal that the small changes in air density barely affect the power generated which follows the wind speed variation, as expected since power is proportional to the cubic of wind speed. The variations in Figures 11 and 12 confirm that the data acquisition within the system records, correctly, the expected trends in the meteorological data as well as the corresponding expected changes in the power produced by the wind turbine.

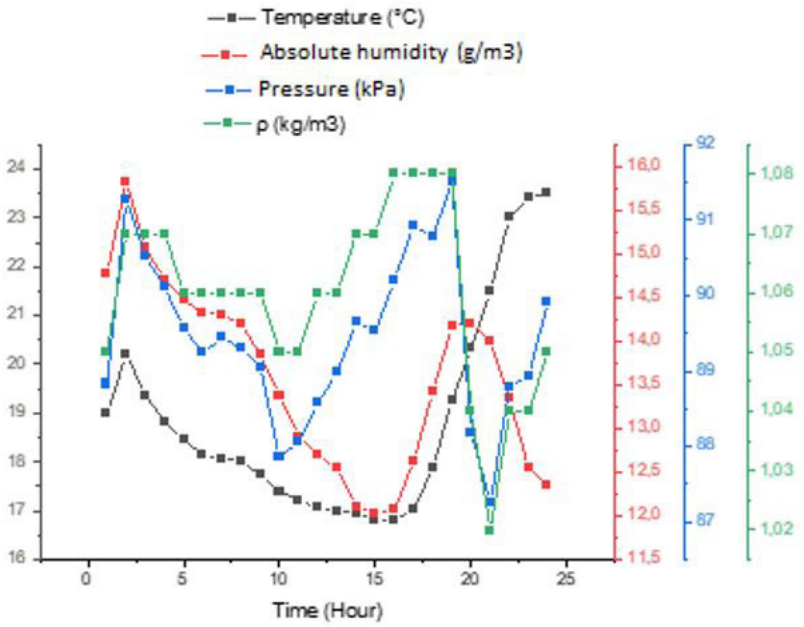

Figure 11: Variations of the absolute humidity, pressure, air density and temperature over a typical 24hr period

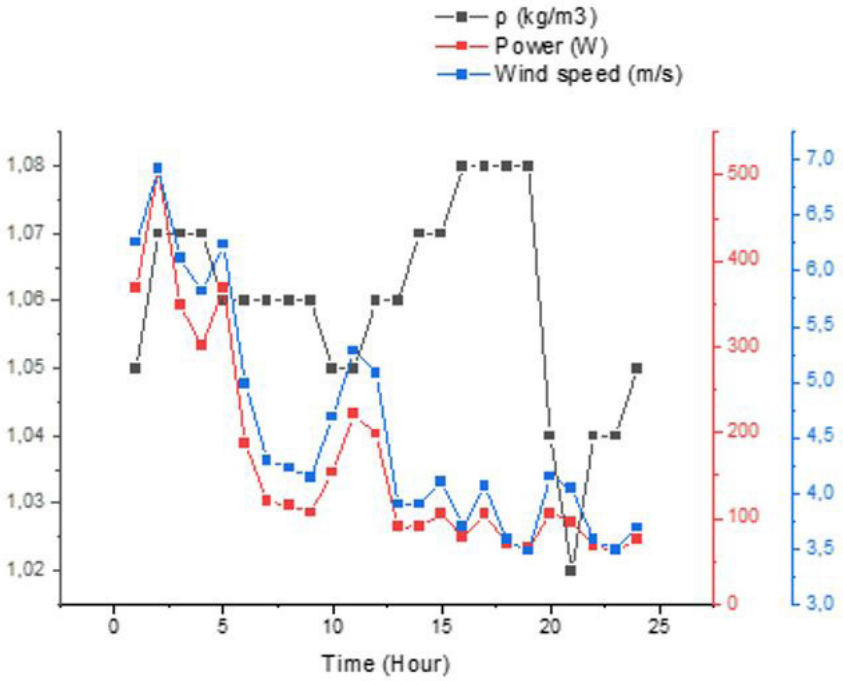

Figure 12: Hourly variations of wind speed, air density, and power produced by wind generator

Data acquisition of operating parameters

Battery Mode

The battery mode is designed in the monitoring algorithm according to the way in which the energy manager has been programmed. The role of this operating mode is to limit the system's power consumption impact when the battery charge level is below 30%. The power manager detects the passage of a mains power to battery power and, depending on the battery charge level, switches automatically to battery mode. Figures 13, 14 and 15 relate to values recorded on May 14 2020 representing, respectively, the batteries voltage level, the three-phase voltage at the output of the wind generator, and the AC voltage at the stand-alone inverter output. Thus, the process of charging the batteries by the wind generator's energy generation was observed, which is confirmed

by the values recorded in Figure 15 where the voltage values reach 20 V. Consequently, the AC voltage at the stand-alone inverter was observed (Figure 15).

From the results presented in Figure 15, it is observed that the batteries storage state is linked to the system's power production and to the batteries state controller output regulation where a quasi-stability for the case of a low energy production is observed (see Figure 15), and an increase in the voltage of batteries was registered when system production occurred. There appears to be some peaks of about 0.1 to 0.2 V that are linked to the controller running mainly due to contractors shunting and opening.

Therefore, from the results presented in Figure 15, it is observed that a poorer production occurs mainly between 1st and 07:30th hours of the measurement. This seems to be linked to the absence of wind velocity. Also, during the rest of the period of measurements the wind velocity varies randomly which may explain the variations observed in the controller voltage input or wind generator voltage output. The results demonstrate successful remote monitoring and operation of the wind energy system allowing automatic switch to battery mode when needed.

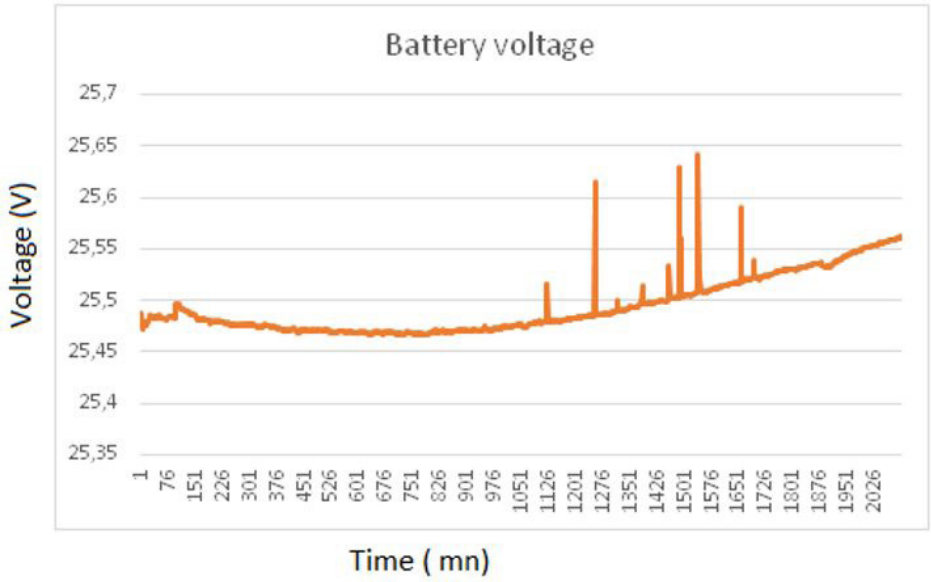

Figure 13: Batteries voltage variation for battery mode operation

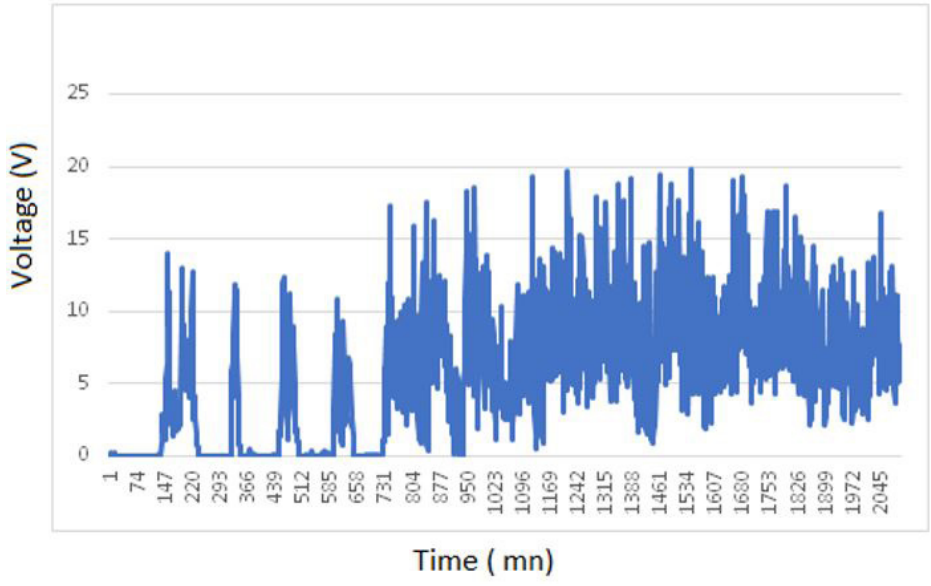

Figure 14: Three phase voltage at the inverter input for battery mode operation

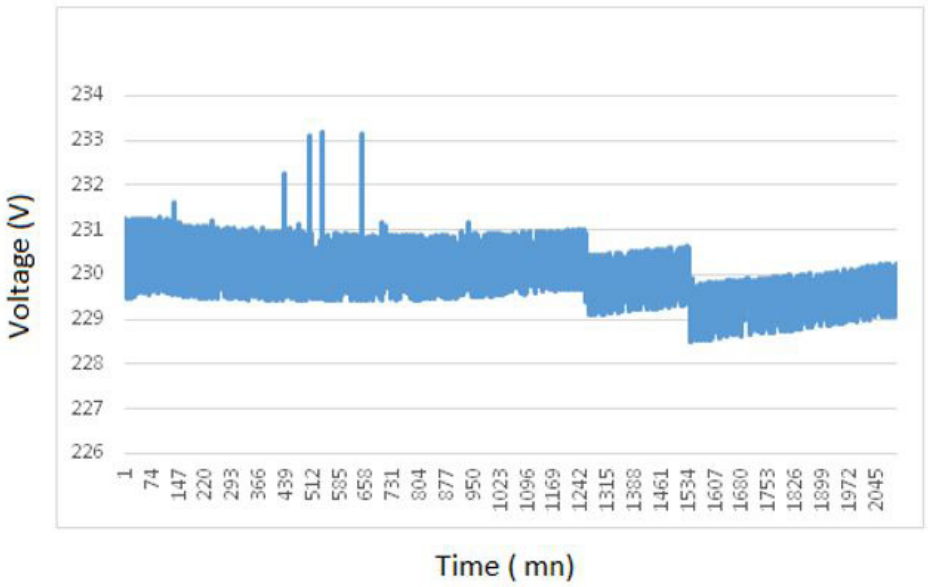

Figure 15: Stand-alone inverter voltage output for battery mode operation

Grid Mode

Similarly, the operation of the system exits "battery mode" to "grid mode" when the energy manager detects that the batteries' state of charge has reached the low threshold. To this end, Figures 16, 17 and 18 present values recorded on June 8 2020, which correspond to grid mode, and are characterized by the unavailability of the wind potential. Thus, it is seen that as soon as the battery voltage reaches 22.5 V (Figure 18), the voltage at the autonomous inverter is zero at the point 169 (Figure 18). This means that during the considered time period the electrical load is supplied only by the grid. These results demonstrate the successful working of the developed system which allows automatic switching to grid mode to ensure continuous supply of electric power when wind energy at the site is unavailable or insufficient for the wind turbine to be operational.

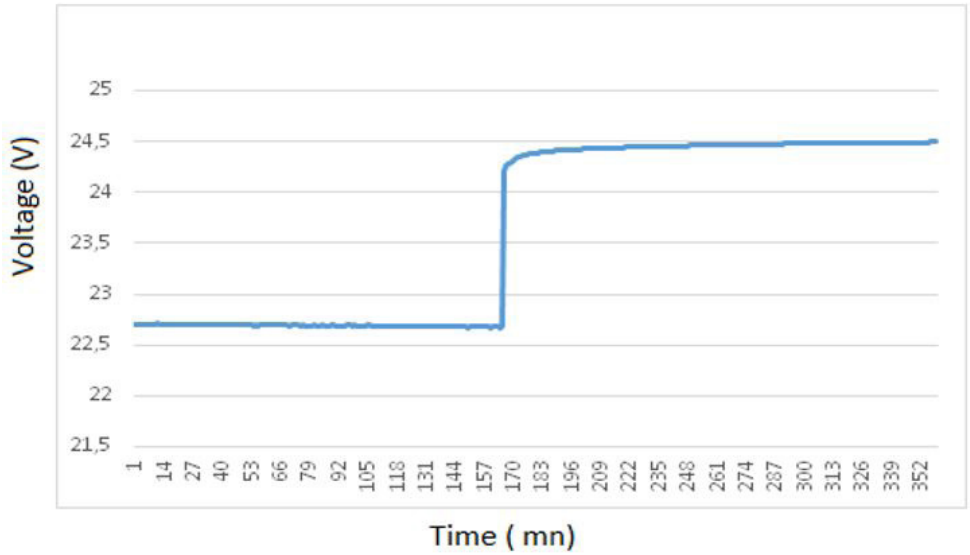

Figure 16: Batteries voltage output for grid mode operation

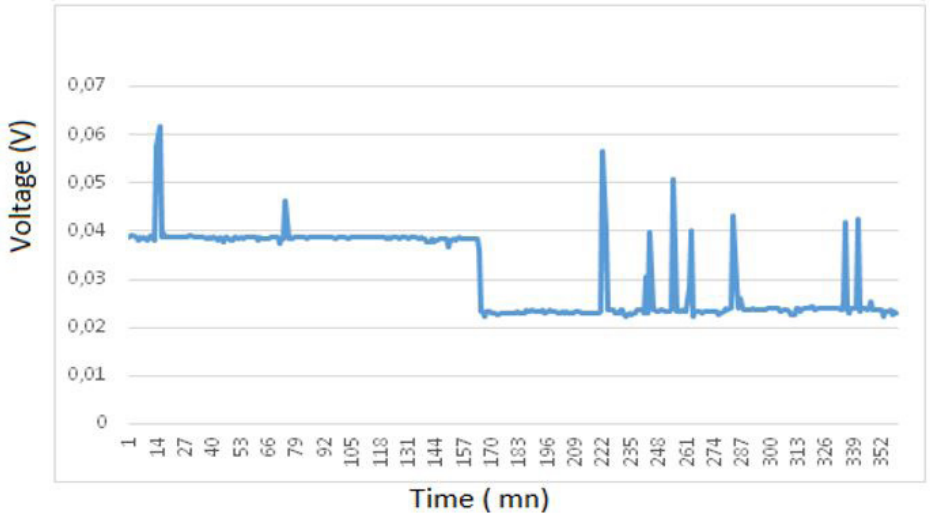

Figure 17: Three phase voltage at the inverter output for grid mode operation

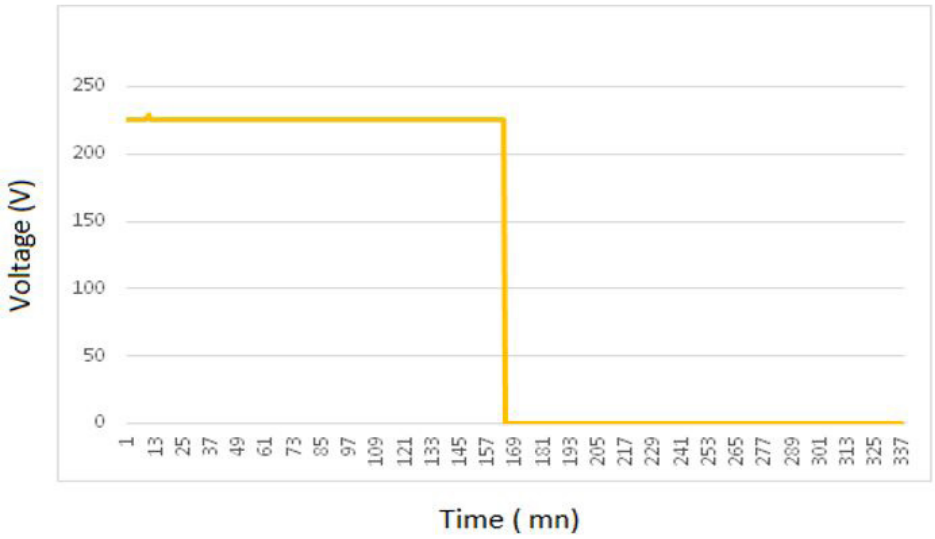

Figure 18: Stand-alone inverter voltage for grid mode operation

The Electric power load effect

In the case of the considered load profile, the system is able to provide lighting on site and at night (Figure 19), supplying power to 10 lamps of 60 W each, and a total AC current of 2.8 A. Again, regarding the load profile and its effect on the system's behavior, two operating modes are taken into account: the battery mode and the grid mode.

Figure 19: Lighting lamp switched on at night using power from the wind generator

Battery Mode

The continuous electrical AC load coverage, achieved via an appropriate inverter of the stand-alone type, is ensured during the autonomy period determined by the battery system as long as the batteries are within the standard load, i.e. greater than 30% of their nominal power as shown in Figure 20.

The voltage and frequency are measured and controlled in real time with precision (Figures 21 ,22) in order to maintain it within an acceptable range (± 0.2 Hz around 50 Hz, corresponding to that of the domestic network which delivers a nominal (effective) voltage of 230 V with a tolerance of +/- 10%, i.e. a range of 207 V to 253 V.

The active and apparent power are also measured in real time, so they can be analyzed in normal time as indicated in Figures 23 and 24. From Figures 23 and 24, it is noticed that the two power curves vary in the same direction, which confirms their dependence on each other, as characterized respectively by 0.168k W to 0.185kW and 0.168 kVA to 0.192 kVA. Thus, these numbers define the amount of energy to be routed to ensure a desired energy for use.

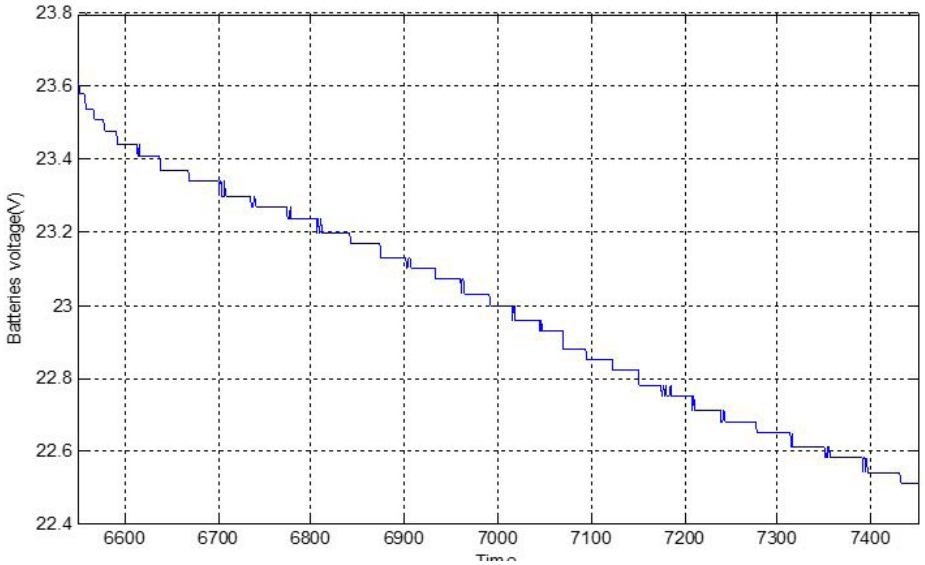

Figure 20: Batteries voltage during the battery mode operation for power load effects

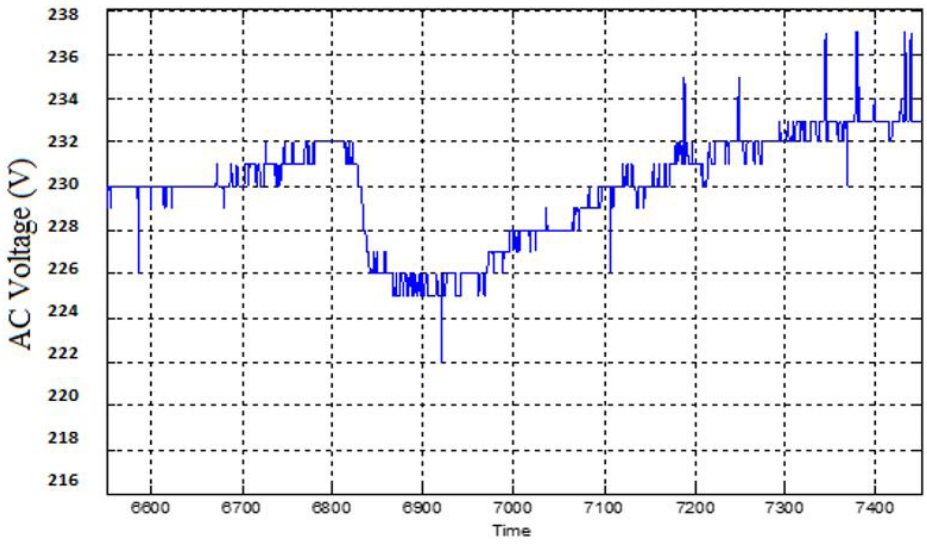

Figure 21: AC voltage during the battery mode operation for power load effects

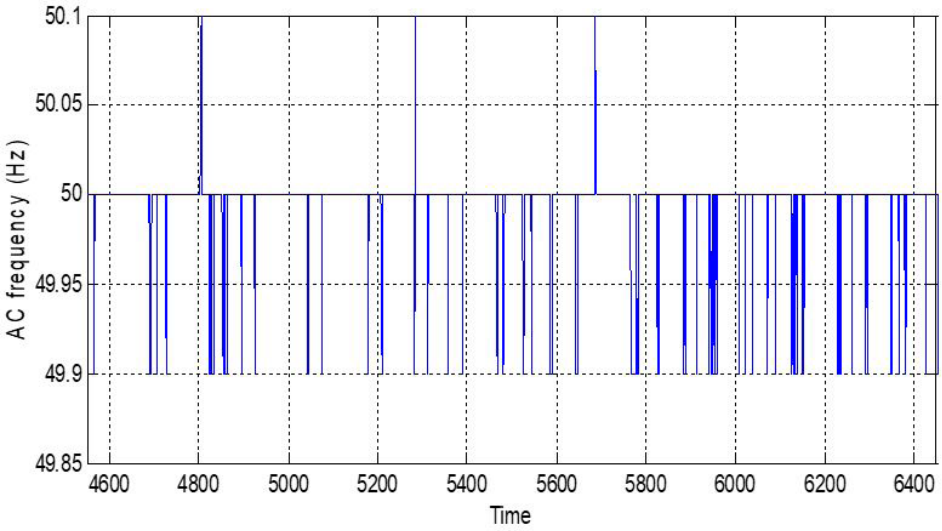

Figure 22: AC frequency during the battery mode operation for power load effects

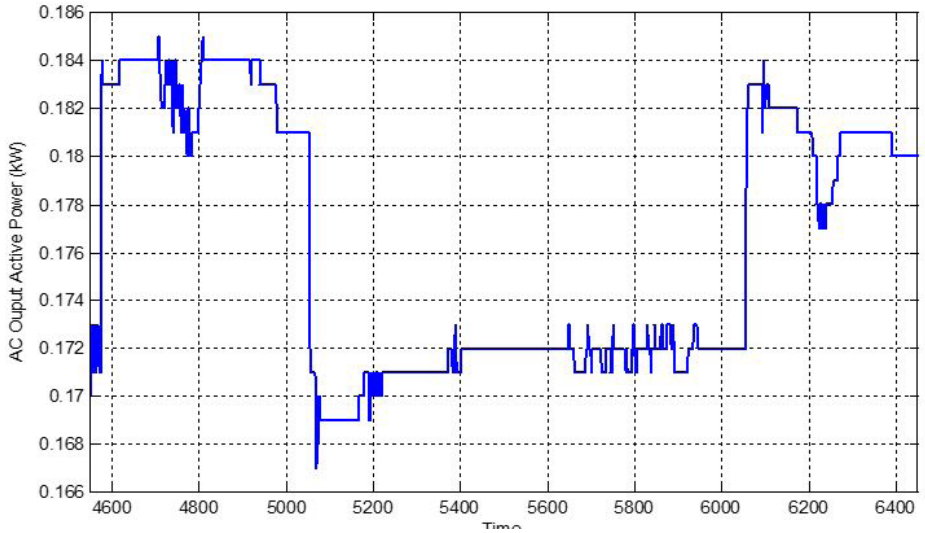

Figure 23: AC Active Power in the battery mode for power load effects

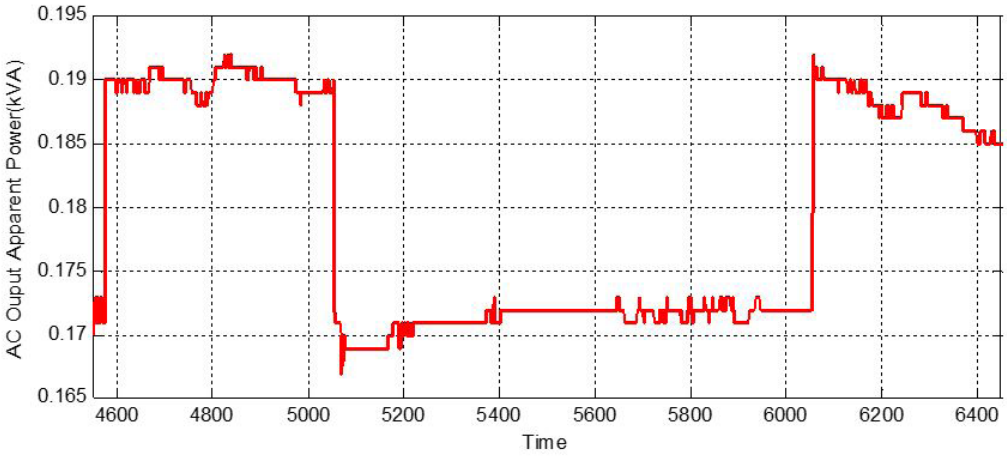

Figure 24: AC active apparent power in the battery mode for power load effects

Grid Mode

In this mode, the grid will provide the electrical coverage to the AC load and charge the batteries via a battery charger. Shown in Figures 25, 26, 27 and 29 are respectively the AC voltage, the frequency, the apparent power and the active power, all corresponding to the data recording made on July 15 2020. It is noticed that the AC voltage values are between 215 V and 238 V which confirms their consistency since the normalized average grid voltage is 230V with a tolerance of +/-10%, i.e. a minimum of 207 V and a maximum of 253 V.

It is also observed that as soon as the voltage exceeds a certain threshold this affects both the apparent and active power (over a duration of 1h 30min to 3h 30min). These last two increase respectively to 50 VA and 20 W. Concerning the frequency, and according to Figure 26, it is seen that it varies between 50 Hz and 50.1 Hz, which confirms that this very slight change does not practically affect the stability of the power grid. Again, all measurements from the remotely monitored wind turbine system confirm correct functioning of the developed setup in terms of the power load effects for both the battery mode and the grid mode.

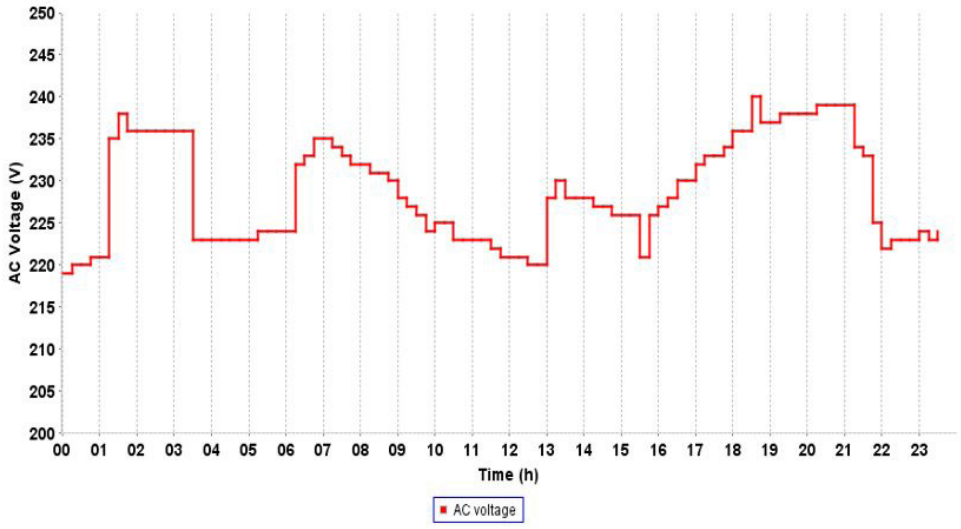

Figure 25: AC voltage in the grid mode for power load effects

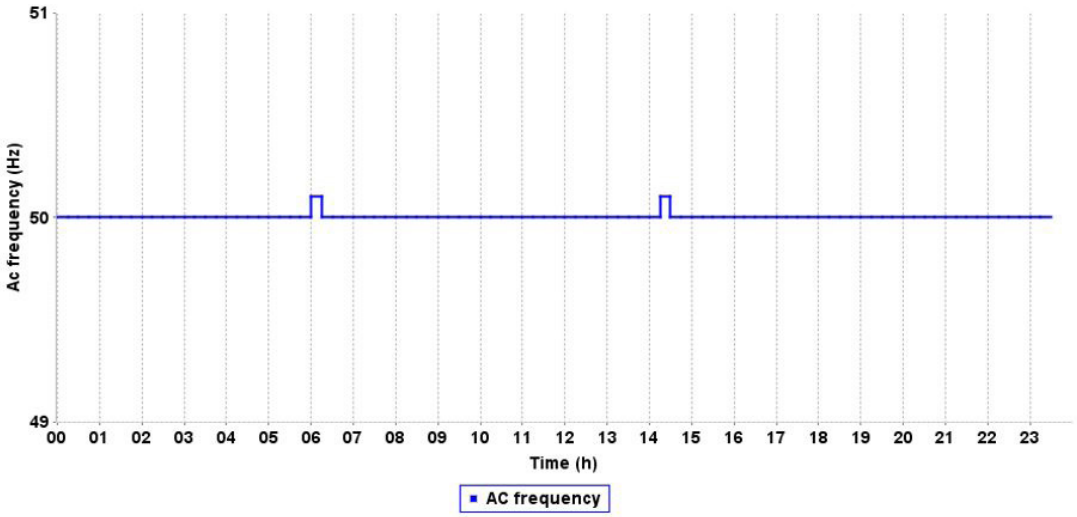

Figure 26: AC frequency in the grid mode for power load effects

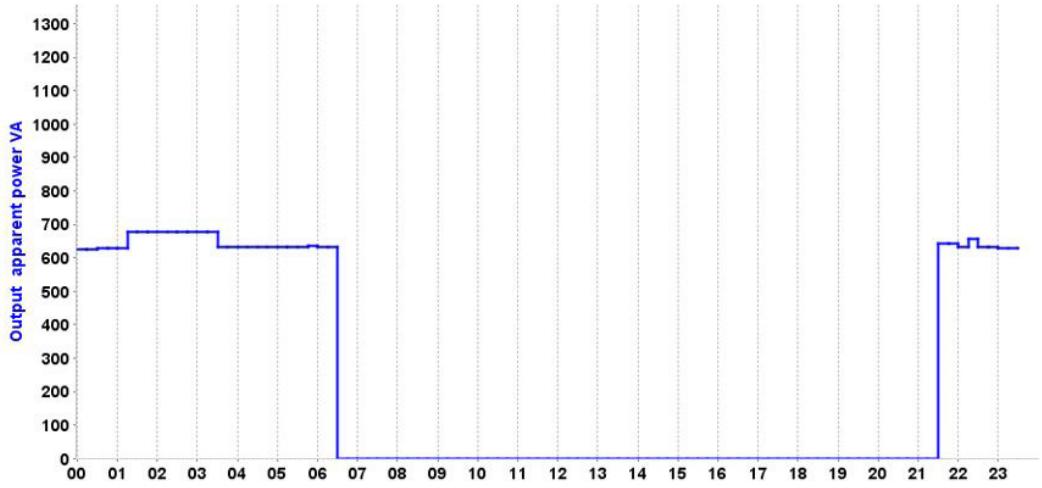

Figure 27: Output Apparent Power in the grid mode for power load effects

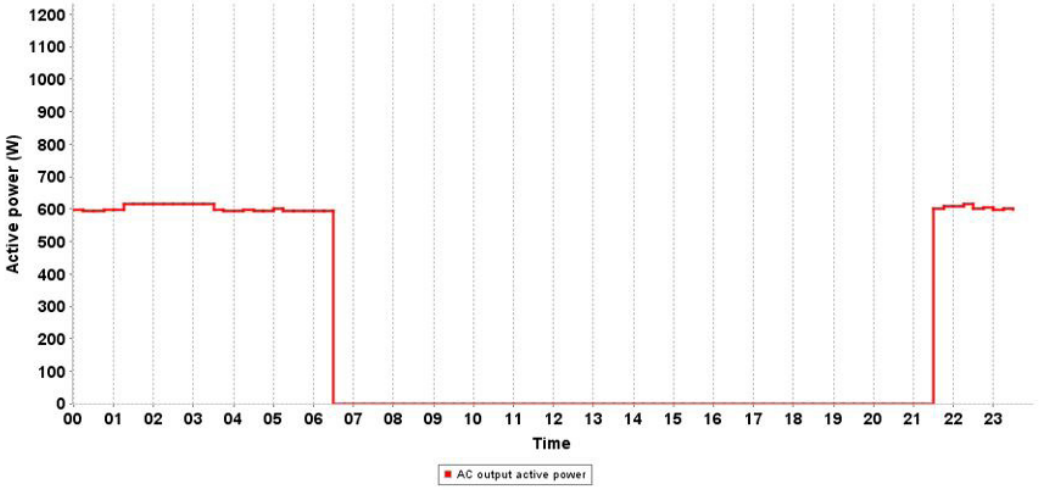

Figure 28: Output Active Power in the grid mode for power load effects

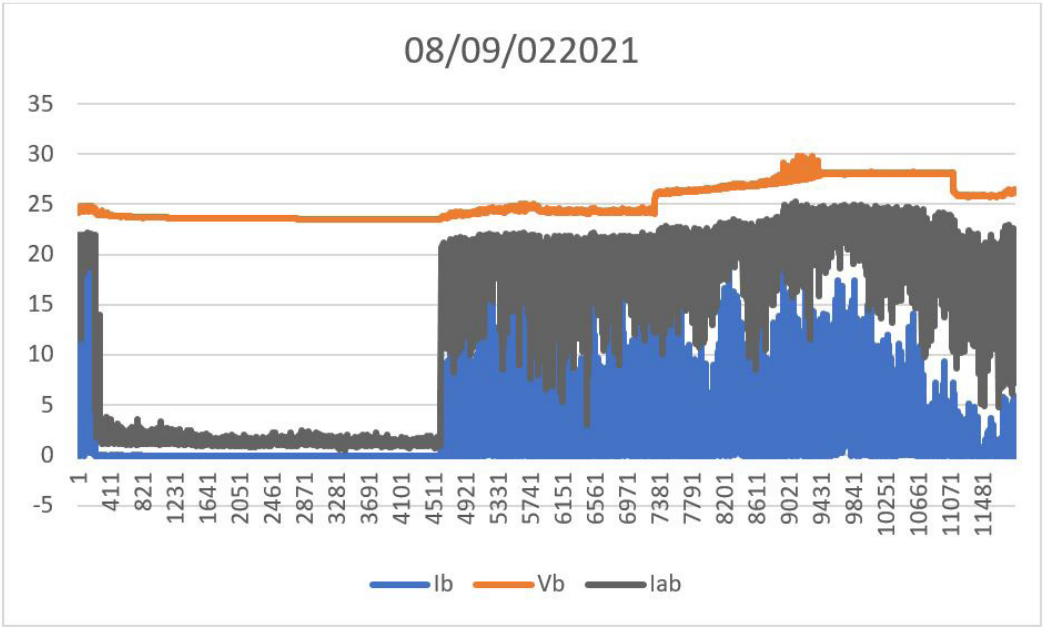

Figure 29: The obtained data registration from 08- 09 February 2021

Conclusions

In this study, a remote monitoring system for a wind generator backed up by the electrical grid and operated via IoT has been designed and successfully implemented onsite at the CDER, Algiers, Algeria. The technical characteristics of the developed system are as follows:

1. It provides permanent information, 24 hours a day, via the Internet and through the easily accessible software AnyDesk. The most important advantage of this software is its fluidity in remote control without slowing for data transfer, thus allowing instantaneous monitoring of the wind energy system;

2. Data acquisition of meteorological parameters show accurate trends, including particularly how power production is affected by variations in the wind characteristics;

3. The system displays the instantaneous parameters of active and reactive power, voltage and frequency as recorded through sensors and data acquisition system AGILENT 34970, and as delivered by the wind turbine and stored in accessible and easy to use Excel files;

4. It displays the instantaneous parameters of the wind speed and direction, ambient temperature, battery temperature, humidity and atmospheric pressure via the meteorological data logger designed and realized at CDER;

5. It presents information using the GUI / MATLAB software, allowing graphical display of information. This is crucial for supervising and controlling power production as well as its timely transfer to storage devices and units in order to optimize the services provided to the end user;

6. The system is able to produce lighting for ten lamps of 60W each, consuming only a total current of 2.8A;

7. The primary source of energy supply is the wind generator / battery system combination.

The obtained results from the developed remotely controlled wind power system demonstrate satisfactory and reliable operation of the developed system for the supervision and acquisition of meteorological data and for the various electrical operating parameters. The findings will be used to observe the behavior of the wind generator constantly, to validate the power curves, to optimize the system's efficiency, and to create a database for further research. The system developed is applicable to not only wind turbine units both small and large scale, but also to renewable energy based systems such as solar PV. Future research will look into such aspects.

References

1.Aktar MA, MM Alam, AQ Al-Amin (2020) Global economic crisis, energy use, CO2 emissions and policy roadmap amid COVID-19. Sustainable Production and Consumption.

2.Camporeale C, R Del Ciello, M Jorizzo (2021) Beyond the Hydrocarbon Economy: The Case of Algeria, in Sustainable Energy Investment- Technical, Market and Policy Innovations to Address Risk, IntechOpen.

3.Priyadarshi N, et al. (2019) An ant colony optimized MPPT for standalone hybrid PV-wind power system with single Cuk converter. Energies 12: 167.

4.Priyadarshi N, Padmanaban S, Bhaskar MS, Blaabjerg F, Holm-Nielsen JB (2019) An improved hybrid PV-wind power system with MPPT for water pumping applications. International Transactions on Electrical Energy Systems 30: 1-26.

5.Yan J, Lu L, Ma T, Zhou Y, Zhao CY (2020) Thermal management of the waste energy of a stand-alone hybrid PV-wind-battery power system in Hong Kong. Energy Conversion and Management 203: 112261.

6.Sanjari MJ, HB Gooi, NKC Nair (2019) Power generation forecast of hybrid PV–Wind system. IEEE Transactions on Sustainable Energy 11: 703-12.

7.Fasihi M, C Breyer (2020) Baseload electricity and hydrogen supply based on hybrid PV-wind power plants. Journal of Cleaner Production 243: 118466.

8.Dhunny AZ, Doorga JRS, Allam Z, Lollchund MR, Boojhawon, R (2019) Identification of optimal wind, solar and hybrid wind-solar farming sites using fuzzy logic modelling. Energy 188: 116056.

9.Adefarati T, RC Bansal (2019) Reliability, economic and environmental analysis of a microgrid system in the presence of renewable energy resources. Applied Energy 236: 1089-114.

10.Hassan MU, Rehmani MH, Kotagiri R, Zhang J, Chen J (2019) Differential privacy for renewable energy resources based smart metering. Journal of Parallel and Distributed Computing 131: 69-80.

11.Murthy K. O Rahi (2017) A comprehensive review of wind resource assessment. Renewable and Sustainable Energy Reviews 72: 1320-42.

12.Malawi PO (2018) Solar Resource Atlas.

13.Boudia SM, JA Santos (2019) Assessment of large-scale wind resource features in Algeria. Energy 189: 116299.

14.Nedjari, H. D., Haddouche, S. D., Balehouane, A., Guerri, O. Optimal windy sites in Algeria: Potential and perspectives. Energy, 2018. 147: p. 1240-1255.

15.Krishan O, S Suhag (2019) Techno-economic analysis of a hybrid renewable energy system for an energy poor rural community. Journal of Energy Storage 23: 305-19.

16.Das M, MAK Singh, A Biswas (2019) Techno-economic optimization of an off-grid hybrid renewable energy system using metaheuristic optimization approaches–case of a radio transmitter station in India. Energy Conversion and Management 185: 339-52.

17.Salhaoui M, Arioua M, Guerrero-González A, García-Cascales MS (2018) An IoT Control System for Wind Power Generators. In: Medina J., Ojeda-Aciego M., Verdegay J., Perfilieva I., Bouchon-Meunier B., Yager R. (eds) Information Processing and Management of Uncertainty in Knowledge-Based Systems. Applications. IPMU, 2018. Communications in Computer and Information Science 855.

18.Zhao L, Zhou Y, Matsuo I, Korkua S, Lee S (2019) The design of a remote online holistic monitoring system for a wind turbine. IEEE Transactions on Industry Applications 56: 14-21.

19.Chandra AA, Jannif NI, Prakash S, Padiachy V (2017) Cloud based real-time monitoring and control of diesel generator using the IoT technology. In 20th International Conference on Electrical Machines and Systems (ICEMS), IEEE.

20.Liew HF, Rosemizi AR, Aihsan MZ, Muzamir I, Baharuddin I (2020) Wind characterization by three blade savonius wind turbine using IoT. In IOP Conference Series: Materials Science and Engineering. IOP Publishing.

21.Karad S, R Thakur (2021) Efficient monitoring and control of wind energy conversion systems using Internet of things (IoT): a comprehensive review. Environment, Development and Sustainability 1-18.

22.Pawar P, M TarunKumar (2020) An IoT based Intelligent Smart Energy Management System with accurate forecasting and load strategy for renewable generation. Measurement 152: 107187.

23.Bedi G, et al. (2018) Review of Internet of Things (IoT) in electric power and energy systems. IEEE Internet of Things Journal 5: 847-70.

24.Djohra SK, Rennane A, Boudraf M, Boufertella A, Koussa MA (2019) Novel Control Strategy using Arduino Grid and Grid Connected Including Wind Generator, Diesel and Battery Storage Plants: Experimental Behavior. In 2019 7th International Renewable and Sustainable Energy Conference (IRSEC) IEEE.

25.Khelifati AB, R Amrani (2019) Réalisation d'une carte d'acquisition des paramètres météorologiques USTHB.

26.El Moustapha SM, Ndiaye Ml, Ndiaye PA, Mahmoud AKO, Youm I (2014) Influence des paramètres météorologiques sur la production d'un aérogérateur. Revue des énergies renouvelables 17: 46-54.